



# PCCP

## The Effect of Co-adsorbed Solvent Molecules on H<sub>2</sub> Binding to Metal Alkoxides

|                               |   |
|-------------------------------|---|
| Journal:                      | <i>Physical Chemistry Chemical Physics</i>  |
| Manuscript ID                 | CP-ART-02-2019-000754.R1  |
| Article Type:                 | Paper   |
| Date Submitted by the Author: | 28-Mar-2019   |
| Complete List of Authors:     | Colon, Yamil; University of Notre Dame, Chemical and Biomolecular Engineering<br>Snurr, Randall; Northwestern University, Department of Chemical & Biological Engineering |
|                               |   |

SCHOLARONE™  
Manuscripts



Journal Name

ARTICLE

## The Effect of Co-adsorbed Solvent Molecules on H<sub>2</sub> Binding to Metal Alkoxides

Yamil J. Colón<sup>a</sup> and Randall Q. Snurr<sup>b\*</sup>Received 00th January 20xx,  
Accepted 00th January 20xx

DOI: 10.1039/x0xx00000x

[www.rsc.org/](http://www.rsc.org/)

The introduction of metal alkoxides has been proposed as an attractive option to enhance hydrogen binding energies in porous materials such as metal-organic frameworks (MOFs) for room-temperature hydrogen storage applications. The presence of residual solvent molecules from MOF synthesis can, however, affect the performance of these functional groups. We perform quantum chemical calculations to predict solvent binding energies onto the metal-alkoxides and the temperatures required to drive off the solvent molecules and successfully activate porous materials with these moieties. Calculations are performed for Li, Mg, Zn, Cu, and Ni alkoxides and chloroform (CHCl<sub>3</sub>), dimethylformamide (DMF), ethanol, methanol, and water solvent molecules. We identify CHCl<sub>3</sub> as a promising solvent that can be removed from these alkoxides at mild temperatures, whereas DMF binds strongly to the metal alkoxides and removal would require temperatures above the present upper bound of thermal stability in MOFs. As a second objective, we calculated the binding energies of hydrogen to metal alkoxide-solvent complexes to explore the effect of any solvent molecules that cannot be removed.

### Introduction

Concerns over environmental consequences of fossil fuels and their finite supply have sparked research into alternative energy sources. Hydrogen has received particular attention as a viable option. Using hydrogen as a source of energy is attractive since it is nontoxic and its oxidation product is water. Further, hydrogen could be used in clean energy systems if the hydrogen is produced from renewable sources. Despite these advantages, the efficient storage of hydrogen has proved to be a significant hurdle for the advent of a hydrogen economy.

An example that highlights the hydrogen storage challenge is the implementation of fuel tanks for vehicular applications.<sup>1-4</sup> It has been estimated that 5-13 kg of H<sub>2</sub><sup>5</sup> are needed as fuel to power a typical automobile. To meet this demand, current efforts to store hydrogen in vehicles employ pressures as high as 700 bar.<sup>5</sup> Honda and Toyota are some of the automobile companies that have hydrogen-powered cars on the road today. These proofs of concept notwithstanding, the high pressure necessary to store the hydrogen fuel creates safety (high pressure gas tanks), economic (compression costs), and design concerns. Materials-based approaches offer an alternative that may overcome these challenges.

In materials-based approaches, hydrogen can interact with a solid material via either chemisorption or physisorption.

Metal hydrides,<sup>6, 7</sup> which utilize chemisorption, are capable of high gravimetric and volumetric uptake, but the hydrogen molecule is dissociated. This impedes the release of hydrogen molecules from the fuel tank to the fuel cell engine since the recombination kinetics of the hydrogen molecule are slow. Further, high temperatures are required to release the hydrogen molecules, and the release process may result in unwanted and harmful side products. Conversely, physisorption offers the advantage of effective release with a simple temperature or pressure swing. Porous materials, in particular, exploit physisorption, and if they contain large void fractions and surface areas, their storage capabilities are attractive, especially at cryogenic temperatures. Hence materials such as metal-organic frameworks (MOFs), nanoporous crystalline structures comprised of inorganic nodes and organic linkers, have been the subject of extensive studies exploring their use in hydrogen storage applications.<sup>8-16</sup> The physisorption interactions, however, are weak, and the hydrogen storage capacity of these materials falters as temperatures approach room temperature.

To strengthen the material-hydrogen interactions and improve the hydrogen storage performance of porous materials, researchers have introduced metals through doping of the material or chemical functionalization in the form of metal catecholates or alkoxides.<sup>17-22</sup> Computational studies indicate that the positive charge on the metal in the various chemical functionalizations interacts favorably with the quadrupole of the hydrogen molecule and increases the interaction strength.<sup>23-29</sup> Studies have also identified promising metal alkoxide candidates and structures that would greatly outperform the hydrogen storage of their unfunctionalized counterparts.<sup>30-37</sup> Experimental studies by Mulfort *et al.*,<sup>19</sup> Himsl *et al.*,<sup>21</sup> and Xiang *et al.*<sup>22</sup> incorporated metal sites into the

<sup>a</sup> Department of Chemical and Biomolecular Engineering, University of Notre Dame, Notre Dame, IN 46556, USA.

<sup>b</sup> Department of Chemical and Biological Engineering, Northwestern University, Evanston, IL 60208, USA.

\*Corresponding author. E-mail: [snurr@northwestern.edu](mailto:snurr@northwestern.edu)

Electronic Supplementary Information (ESI) available: Comparison between different levels of theory, tabulated values for binding energies and solvent release temperatures, and coordinates of optimized geometries.

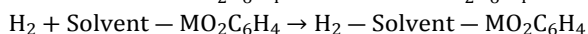
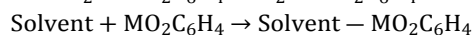
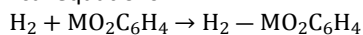
framework using metal alkoxides (Li and Mg). The functionalized structures show improved hydrogen storage and heats of adsorption at cryogenic temperatures. As these open metal sites interact strongly with hydrogen molecules, it is reasonable to think interactions with solvent molecules — which may be left over from synthesis or may be impurities in a gas stream — will also be strong. It is important to understand the interactions between solvent molecules and metal alkoxides and the effect they might have on the resulting hydrogen adsorption. In recent work, Tsvion and co-workers studied the effect that a residual solvent molecule bound to the metal can have on hydrogen physisorption onto Mg and Ca alkoxides. The authors found that the presence of the solvent can significantly weaken the binding energy onto Mg alkoxide and to a lesser degree Ca alkoxide.<sup>38</sup>

To find solvent-metal alkoxide pairs that allow for proper activation, we use quantum chemical calculations to assess and characterize the binding of typical solvent molecules (chloroform, dimethylformamide, ethanol, methanol, and water) used in the synthesis of MOFs onto different metal alkoxides (Li, Mg, Zn, Cu, Ni). We also estimate the temperatures required to remove the solvent molecules from the metal alkoxides. Recognizing that some solvent molecules may not be completely removed, we calculate the binding energies for hydrogen onto solvent-metal alkoxide complexes to find systems that bind hydrogen at the desired energy.

## Methods

Electronic structure calculations were performed with the Gaussian 09 software, revision D.<sup>39</sup> The calculations were performed self-consistently and convergence was considered to be achieved when the change in the density matrix and change in electronic energy between consecutive iterations was less than  $10^{-6}$  Å<sup>-3</sup> and  $10^{-6}$  Ha, respectively. Geometries were considered converged when the maximum atomic force, root-mean squared force, maximum displacement and root mean squared displacement were below  $4.5 \times 10^{-4}$  Ha/Å,  $3.0 \times 10^{-4}$  Ha/Å,  $1.8 \times 10^{-3}$  Å, and  $1.2 \times 10^{-3}$  Å, respectively.

As in previous studies,<sup>28, 33, 38</sup> we approximated a full MOF linker by a single aromatic ring with an attached alkoxide as shown in Figure 1 (also referred to as a metal catecholate in the literature). Three sets of binding energies were calculated: hydrogen onto metal alkoxide, solvent onto metal alkoxide, and hydrogen onto solvent-metal alkoxide complex. Each geometry optimization of the complexes was performed using three different initial configurations, and the lowest energy configuration is reported. Frequency analysis was used to confirm that the configurations are local minima and do not have any imaginary frequencies. Binding energies were calculated by subtracting the electronic energies of the isolated reactants from the electronic energy of the product in the following chemical equations:



where M is either Li, Mg, Zn, Cu, or Ni (when Li is the metal species, the formula of the chemical formula is LiOC<sub>6</sub>H<sub>5</sub>), and "Solvent" is chloroform (CHCl<sub>3</sub>), dimethylformamide (DMF), ethanol, methanol, or water (H<sub>2</sub>O). As illustrated in Figure 1, calculating the hydrogen binding energy onto a Mg alkoxide, for example, would entail calculating the difference between the hydrogen-metal alkoxide complex electronic energy and the sum of the electronic energies of the isolated hydrogen molecule and isolated Mg alkoxide: Binding energy =  $E(\text{H}_2 - \text{MgO}_2\text{C}_6\text{H}_4) - E(\text{H}_2) - E(\text{MgO}_2\text{C}_6\text{H}_4)$ .

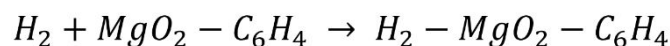
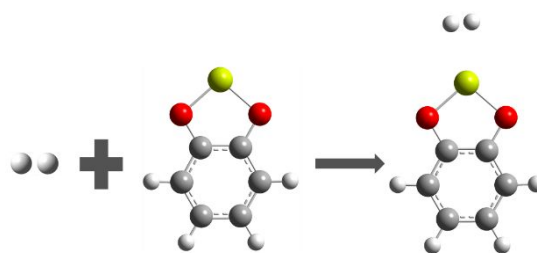


**Figure 1.** Illustration of hydrogen binding energy calculation. The individual energies of the hydrogen molecule and the Mg alkoxide are subtracted from the energy of the hydrogen-Mg alkoxide complex to obtain the hydrogen binding energy onto the Mg alkoxide. H=white, O=red, Mg=yellow, C=gray.

Geometry optimizations and energies were calculated at the MP2/6-311+G\*\* (Li, Mg, Zn) or M06<sup>40</sup>/6-311++G\*\* (Cu, Ni) levels of theory. Counterpoise corrections<sup>41</sup> were applied to the MP2/6-311+G\*\* results to offset basis-set superposition errors. Previous studies showed that for Cu and Ni catecholates, where hydrogen binding is very strong, M06 gives comparable results to MP2 and is much faster.<sup>33, 34</sup> As a reference, we calculated all solvent binding energies for Zn alkoxide with both MP2 and M06 and compare their results in Table S1. The resulting binding energies are in reasonable agreement (within 15%).

For the MP2 calculations of the H<sub>2</sub> binding energy onto the solvent/metal alkoxide, three fragments (H<sub>2</sub>, solvent, and metal alkoxide) are considered for the counterpoise corrections. To obtain the binding energy, the energies of the individual fragments (hydrogen molecule, solvent, and metal alkoxide) and the counterpoise-corrected binding energy of the Solvent - MO<sub>2</sub>C<sub>6</sub>H<sub>4</sub> complex are subtracted from the counterpoise-corrected energy of the H<sub>2</sub> - Solvent - MO<sub>2</sub>C<sub>6</sub>H<sub>4</sub> complex. For the M06 calculations, the energies of the H<sub>2</sub> molecule and the Solvent - MO<sub>2</sub>C<sub>6</sub>H<sub>4</sub> complex are subtracted from the energy of the H<sub>2</sub> - Solvent - MO<sub>2</sub>C<sub>6</sub>H<sub>4</sub> complex to obtain the H<sub>2</sub> binding energy onto the solvent/metal alkoxide complex.

Solvent-release temperatures were estimated from the free energies for solvent adsorption:<sup>42</sup>

$$\Delta G_{\text{adsorption}} = G_{\text{Solvent-Alkoxide}} - G_{\text{Alkoxide}} - G_{\text{Solvent}}$$

The solvent release temperature was estimated to be the temperature where the free energy of adsorption is zero. In calculating the free energies, vibrational frequencies below 25 cm<sup>-1</sup> were set equal to 25 cm<sup>-1</sup>.

Natural bond orbital (NBO)<sup>43</sup> analysis was performed to characterize and visualize the solvent-metal alkoxide

interactions.<sup>44</sup> Natural Coulomb electrostatic (NCE) analysis was also performed to characterize the Lewis and non-Lewis character of the binding interactions between solvent and metal alkoxide molecules.<sup>45</sup>

## Results

We validated our calculations by reproducing previously reported values from our group and others<sup>28, 33, 34, 38</sup> for the H<sub>2</sub> binding energy; Table 1 reports the results. Binding energies onto Mg alkoxide reported by other researchers are -23 kJ/mol<sup>30</sup> and -24 kJ/mol<sup>38</sup> calculated at different levels of theory. Our results are in excellent agreement (within 2 kJ/mol) of the literature results. Li has the smallest binding energy at -9.8 kJ/mol, while Ni has the largest binding energy at -84.3 kJ/mol. As described above, calculations for Li, Mg, and Zn alkoxides were performed with MP2, while calculations for Cu and Ni used M06.

**Table 1.** H<sub>2</sub> binding energy onto metal alkoxides: Li, Mg, Zn (MP2), Cu, and Ni (M06).

| Metal-Alkoxide | Binding Energy (kJ/mol) |
|----------------|-------------------------|
| Li             | -9.8                    |
| Mg             | -22.0                   |
| Zn             | -29.4                   |
| Cu             | -83.4                   |
| Ni             | -84.3                   |

Solvent binding energies are reported in Table 2 and Figure 2. The geometries are reported in the SI. As for the H<sub>2</sub> binding energy calculations, MP2 was used for Li, Mg, and Zn metal-alkoxides, while M06 was used for Cu and Ni. The smallest calculated binding energy was for CHCl<sub>3</sub> on Li alkoxide, and the largest was for DMF on Mg alkoxide. For a given metal alkoxide (Figure 2, top panel), solvent molecules bind in the following order: DMF > ethanol > methanol > H<sub>2</sub>O > CHCl<sub>3</sub>. The range of binding energies is largest for Mg and Zn alkoxides and smallest for the Cu alkoxide. For a given solvent (Figure 2, bottom panel), Li alkoxide has the smallest binding energy, while Mg or Ni alkoxides show the largest binding energies in most cases.

**Table 2.** Solvent binding energies on metal alkoxides.

| Solvent           | Binding Energy (kJ/mol) |        |        |        |        |
|-------------------|-------------------------|--------|--------|--------|--------|
|                   | Li                      | Mg     | Zn     | Cu     | Ni     |
| CHCl <sub>3</sub> | -42.6                   | -76.5  | -73.8  | -88.4  | -109.8 |
| DMF               | -97.3                   | -187.9 | -166.8 | -120.6 | -178.1 |
| Ethanol           | -80.9                   | -149.0 | -134.8 | -106.7 | -153.9 |
| Methanol          | -79.7                   | -144.9 | -127.4 | -100.4 | -147.8 |
| H <sub>2</sub> O  | -73.6                   | -127.3 | -110.3 | -91.8  | -138.2 |

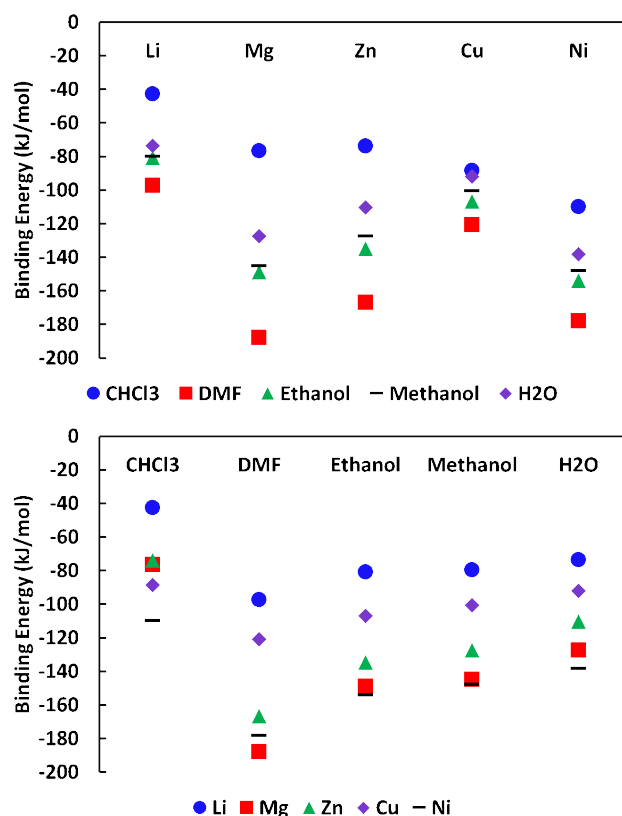


**Figure 2.** Solvent binding energies on metal alkoxides. CHCl<sub>3</sub> has the smallest binding energies, while DMF has the largest. Similarly, Li alkoxide has the smallest binding energies, while Ni and Mg alkoxides have the largest in most cases.

The free energy of solvent adsorption was calculated as a function of temperature from the optimized solvent/metal alkoxide complexes. Then, the temperature at which the free energy of adsorption is unfavorable can be determined. These solvent release temperatures are reported in Figure 3 and Table S2. The overall trends observed are similar to those for the solvent/metal alkoxide binding energies, with solvent release temperatures for the various metal alkoxides ranked in the following order (Figure 3): DMF > Ethanol ~ Methanol ~ H<sub>2</sub>O > CHCl<sub>3</sub>. For a given solvent (Figure S1), Mg alkoxide has the highest solvent release temperature, with the exception of CHCl<sub>3</sub>, where Ni alkoxide has the highest release temperature. Li has the lowest solvent release temperature for all solvents except DMF, where Cu alkoxide has the lowest temperature. Notably, the highest CHCl<sub>3</sub> solvent release temperature is ~ 600 K, while the lowest is close to room temperature.

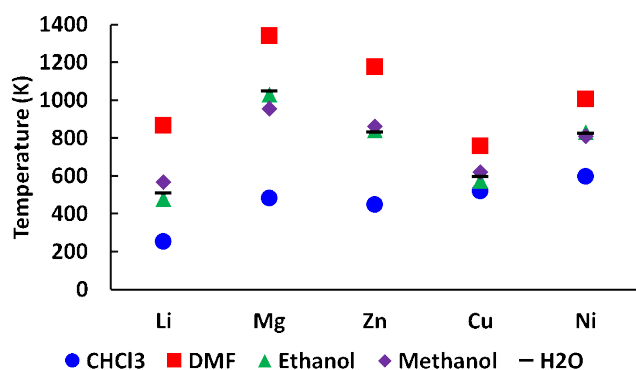


**Figure 3.** Solvent release temperatures for solvent molecules on metal alkoxides. DMF has the highest solvent release temperatures, while CHCl<sub>3</sub> has the lowest. In general, Mg alkoxide has the highest solvent release temperatures, while Li alkoxide has the lowest.

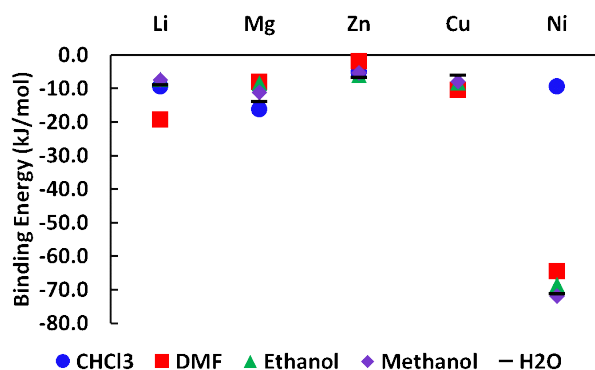


**Figure 4.** H<sub>2</sub> binding energies onto solvent/metal alkoxide complexes. In general, Ni alkoxide has the largest H<sub>2</sub> binding energies. DMF bound to Zn has the smallest H<sub>2</sub> binding energy, while methanol bound to Ni shows the largest H<sub>2</sub> binding energy.

The energies for hydrogen binding with the solvent-metal alkoxide complexes are reported in Figure 4 and Table S3. The geometries are also reported in the SI. The adsorbed solvent molecules occupy the part of the metal site that the H<sub>2</sub> molecule would ideally occupy. Nevertheless, we observe that the hydrogen molecule can still interact with the metal of the alkoxide. In most cases, the hydrogen molecule interacts with the metal species, the oxygen of the alkoxide, and the solvent molecule. Comparing with Table 1, we see that hydrogen binding energies are decreased when a solvent is present on all of the metal alkoxides, with the exception of Li alkoxide with DMF. The weakest hydrogen binding energy is found with the DMF/Zn alkoxide complex, while the hydrogen strength of interaction is highest with the methanol/Ni complex. Notably, Ni alkoxide has the strongest interaction with hydrogen in four out of the five solvent molecules: DMF, ethanol, methanol, and H<sub>2</sub>O, and the binding energies for Ni are significantly stronger than the other metals. We also find complexes that in the presence of a solvent molecule have hydrogen binding energies approximating the desired 20 kJ/mol for reversible hydrogen uptake near room temperature.<sup>23, 28, 29, 33, 36</sup> The DMF/Li and CHCl<sub>3</sub>/Mg alkoxide complexes have hydrogen binding energies of 19.2 kJ/mol and 16.2 kJ/mol, respectively.

## Discussion

After a porous material is synthesized, it is activated, typically by applying high temperature to drive off solvent molecules that remain from the synthesis procedure. Solvent molecules may bind very strongly to metal alkoxides, requiring higher-than-usual temperatures to expose the metal and take advantage of its favorable interactions with an adsorbate of interest, such as hydrogen. As Figure 5 shows, a larger solvent binding energy results in a higher solvent release temperature. The majority of solvent release temperatures lie above 750 K, the current upper bound for thermal stability of MOFs,<sup>46</sup> but there are many systems where it is predicted that the solvent could be released below 750 K. None of the alkoxides with bound DMF have a solvent release temperature below 750 K, but all of the alkoxides with bound CHCl<sub>3</sub> have solvent release temperatures below 750 K. For Li and Cu alkoxides, all of the solvents except DMF show release temperatures below 750 K. For Mg, Zn, and Ni alkoxides, only CHCl<sub>3</sub> has a release temperature below 750 K. This analysis identifies favorable solvent/metal alkoxide combinations that may allow full activation of the material so that hydrogen molecules, or other adsorbates of interest, can interact with the exposed metal of the alkoxide moiety. The solvent/metal alkoxide complexes with solvent release temperatures below 750 K are CHCl<sub>3</sub>/Ni, CHCl<sub>3</sub>/Mg, CHCl<sub>3</sub>/Zn, CHCl<sub>3</sub>/Cu, CHCl<sub>3</sub>/Li, ethanol/Cu, H<sub>2</sub>O/Cu, methanol/Cu, ethanol/Li, H<sub>2</sub>O/Li, and methanol/Li.

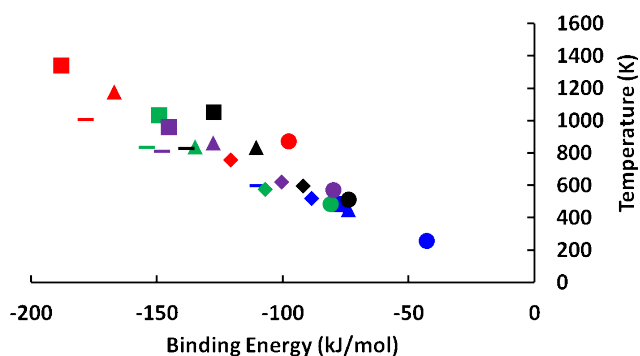


**Figure 5.** Solvent release temperature versus solvent binding energy. Stronger binding energies result in a higher solvent release temperature. Li, Mg, Zn, Cu, and Ni are represented by circles, squares, triangles, diamonds, and dashes, respectively.  $\text{CHCl}_3$ , DMF, ethanol, methanol, and  $\text{H}_2\text{O}$  are represented by the colors blue, red, green, purple, and black, respectively. All complexes containing DMF, red symbols, show solvent release temperatures higher than 750 K, while all complexes containing  $\text{CHCl}_3$ , blue symbols, show temperatures below 750 K. The majority of Li (circles) and Cu (diamonds) alkoxide complexes have solvent release temperatures below 750 K, while the majority of Mg, Zn, and Ni alkoxide complexes have solvent release temperatures above 750 K.

For room temperature hydrogen storage, the desired hydrogen binding energy is approximately 20 kJ/mol. We seek either 1) a system where the solvent can be removed at moderate temperature and hydrogen binds to the (bare) metal alkoxide with an energy near 20 kJ/mol or 2) a system where hydrogen binds to the solvent-metal alkoxide complex with an energy near 20 kJ/mol. Previous studies identified (bare) Mg alkoxide as a promising candidate for hydrogen storage.<sup>33, 34</sup> For Mg, the only solvent molecule that can be released at a temperature lower than 750 K is  $\text{CHCl}_3$ , which would allow for proper activation in MOFs. Additionally, our results show that even with a bound  $\text{CHCl}_3$  molecule, the  $\text{H}_2$  binding energy onto the  $\text{CHCl}_3/\text{Mg}$  alkoxide is still close to 20 kJ/mol. This makes  $\text{CHCl}_3/\text{Mg}$  a good combination for reversible hydrogen uptake at ambient conditions since it would allow for activation below 750 K and shows a hydrogen binding energy close to the desired 20 kJ/mol, even if the solvent is present.

Hydrogen molecules bind favorably with metal alkoxides due to the cationic nature of the open metal.<sup>23, 25, 33</sup> The positive charge interacts favorably with the hydrogen quadrupole, which leads to strong binding energies. To check if these Coulombic contributions also play a role in the metal interactions with solvent molecules, we performed a Natural Coulomb electrostatic (NCE) analysis of the solvent binding interactions. NCE provides information on the Lewis and non-Lewis contributions to the Coulombic interactions. The Lewis contribution is the intermolecular potential energy based on the idealized Lewis structure of the complex. The non-Lewis contribution is a measure of the intermolecular charge transfer, which alters the idealized Lewis picture. Figure 6 shows the results. The total NCE energy is weakest with  $\text{CHCl}_3$  for each alkoxide, while the strongest interactions are with DMF. This coincides with the relative values of their dipole moments:

$\text{CHCl}_3$  has the lowest, while DMF has the highest. Interestingly, Li, Cu, and Ni alkoxides show the weakest Coulombic interactions with solvent molecules, while Mg and Zn show the strongest. The strong Coulombic interactions explain the strong binding energies calculated for Mg and Zn for all solvents, except  $\text{CHCl}_3$  (Figure 2).

The Lewis part of the NCE energy (Figure 6c, d) shows very similar trends to the total NCE energy (Figure 6a, b). For the non-Lewis NCE energy (Figure 6e, f), all solvent molecules show similar trends across the different metals, except for DMF, which exhibits a different trend. DMF shows significantly higher energies than the other solvents for all of the alkoxides, demonstrating that DMF has higher intermolecular charge transfer with the metal alkoxides compared to the other solvent molecules, which explains why DMF has significantly stronger binding energies with all of the alkoxides when compared to the other solvent molecules (Figure 2).



Journal Name

ARTICLE

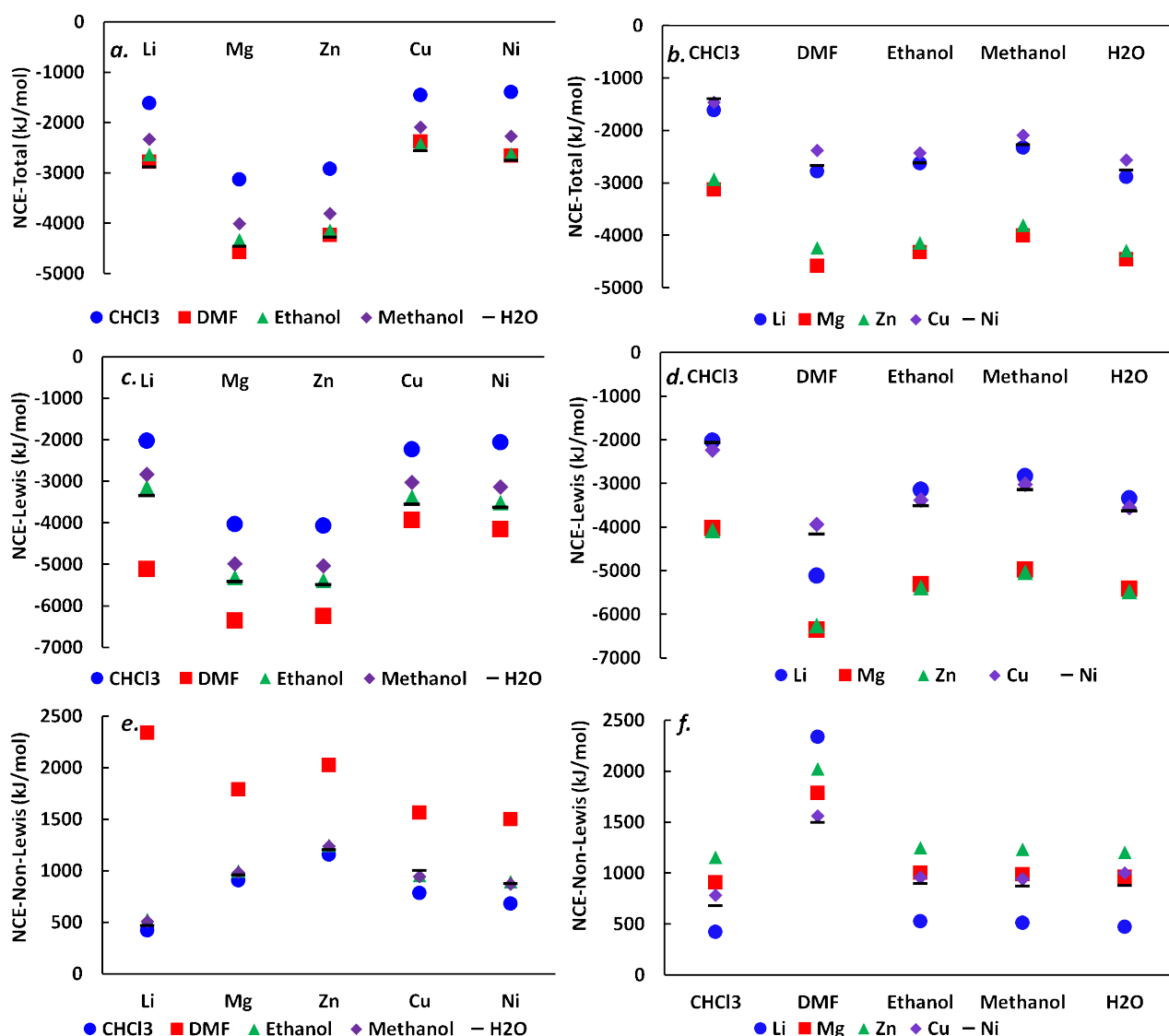


**Figure 6.** NCE analysis for solvent/metal alkoxide complexes. Panels a and b show the total NCE energy, panels c and d show the Lewis contribution to the NCE energy, and panels e and f show the non-Lewis contribution to the NCE energy. DMF has the strongest non-Lewis contribution to the NCE energy, indicating it has the most intermolecular charge transfer.

We also performed a Natural bond orbital (NBO) analysis to visualize the orbitals involved in the interaction between the solvents and the metal-alkoxides. The NBO analysis reveals that all of the interactions involve the Lewis valence lone pair NBO of the solvent as the donor, which interacts with the Lewis acid metal as the acceptor. As Figure 7 shows, the solvent molecules interact with the metal alkoxide through the most electronegative atom of the solvent: chlorine for CHCl<sub>3</sub> and oxygen for DMF, ethanol, methanol, and water. For CHCl<sub>3</sub>, a

chlorine atom interacts with the metal of the alkoxide and the hydrogen atom interacts with an oxygen atom of the alkoxide; the exception is Ni alkoxide, where two chlorine atoms interact with Ni, instead of one. Ethanol, methanol and DMF all have similar interactions across the metal alkoxides. H<sub>2</sub>O interacts “head-on” with Mg and Zn alkoxides while at an angle for Cu and Ni alkoxides. For Li alkoxide, H<sub>2</sub>O induces the Li atom to bend out of plane with the benzene ring.

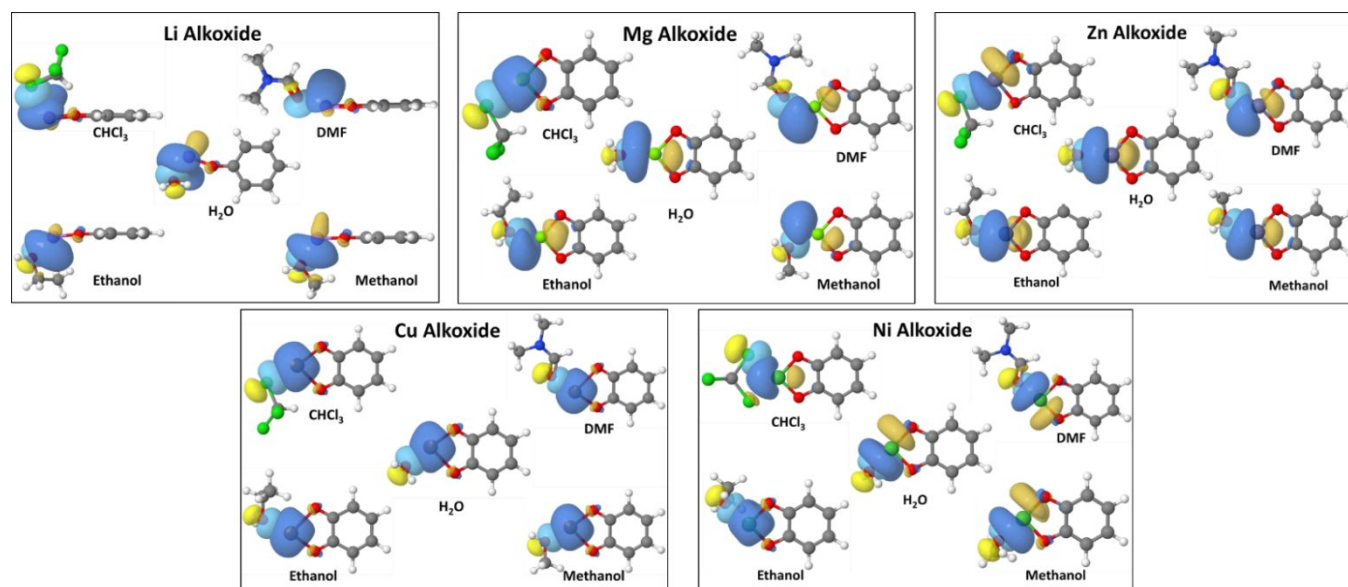


**Figure 7.** NBO analysis for solvent/metal alkoxide complexes. Solvent molecules interact with the metal through the most electronegative atom of the solvent: chlorine for  $\text{CHCl}_3$  and oxygen for DMF, ethanol, methanol, and water. Orbitals shown represent the Lewis valence lone pair NBO of the solvent as the donor interacting with the Lewis acid metal as the acceptor. Blue and yellow clouds represent different phases of the orbitals on each species. C=gray, O=red, H=white, Cl=light green, Li = light purple, Mg = yellow-green, Zn = purple, Cu = orange, and Ni = green.

## Conclusions

Quantum mechanical calculations were performed to calculate  $\text{H}_2$  binding energies on metal alkoxides (Li, Mg, Zn, Cu, and Ni) with and without co-adsorbed solvent molecules ( $\text{CHCl}_3$ , DMF, ethanol, methanol, and water). Binding energies for the solvent molecules were also calculated. Solvent molecules bind on metal alkoxides in the following order of strength: DMF > ethanol > methanol >  $\text{H}_2\text{O}$  >  $\text{CHCl}_3$ . We also estimated the temperatures required to drive off the solvent molecules. The temperatures correlate with the solvent binding energies. All of the complexes containing  $\text{CHCl}_3$  have a solvent release temperature below 750 K, the current upper bound for thermal stability in MOFs. Likewise, all complexes containing DMF have a solvent release temperature above 750 K. Li and Cu alkoxides are predicted to have solvent release temperatures below 750 K for  $\text{CHCl}_3$ , ethanol, water, and methanol, suggesting that they are promising candidates for experimental realization and testing of metal-alkoxides in MOFs.  $\text{CHCl}_3/\text{Mg}$  and DMF/Li are interesting candidates, since the alkoxide/solvent combinations have a hydrogen binding energy close to the desired 20 kJ/mol.

## Conflicts of interest

R.Q.S. has a financial interest in the startup company NuMat Technologies, which is seeking to commercialize metal-organic frameworks.

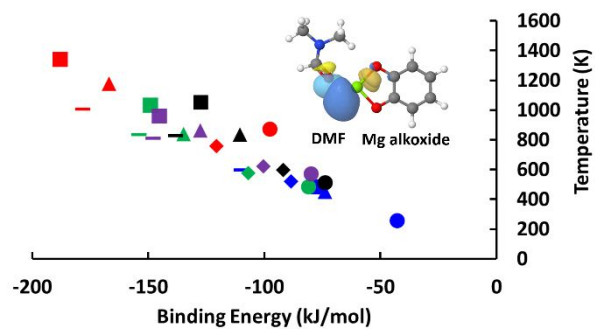
## Acknowledgements

This work was supported by the U.S. Department of Energy under Award DE-FG02-08ER15967.

## Notes and references

1. L. Schlapback and A. Züttel, *Nature*, 2001, **414**, 353.
2. S. W. Jorgensen, *Current Opinion in Solid State and Materials Science*, 2011, **15**, 39-43.
3. W. I. F. David, *Faraday Discussions*, 2011, **151**, 399-414.
4. P. Jena, *The Journal of Physical Chemistry Letters*, 2011, **2**, 206-211.
5. DOE(US), *Hydrogen Storage*, <https://www.energy.gov/eere/fuelcells/hydrogen-storage>.

6. B. Sakintuna, F. Lamari-Darkrim and M. Hirscher, *International Journal of Hydrogen Energy*, 2007, **32**, 1121-1140.
7. E. S. Cho, A. M. Ruminski, Y.-S. Liu, P. T. Shea, S. Kang, E. W. Zaia, J. Y. Park, Y.-D. Chuang, J. M. Yuk, X. Zhou, T. W. Heo, J. Guo, B. C. Wood and J. J. Urban, *Advanced Functional Materials*, 2017, 1704316.
8. J. L. C. Rowsell and O. M. Yaghi, *Angew. Chem. Int. Ed.*, 2005, **44**, 4670-4679.
9. L. J. Murray, M. Dinca and J. R. Long, *Chemical Society Reviews*, 2009, **38**, 1294-1314.
10. O. K. Farha, A. O. Yazaydin, I. Eryazici, C. D. Malliakas, B. G. Hauser, M. G. Kanatzidis, S. T. Nguyen, R. Q. Snurr and J. T. Hupp, *Nature Chemistry*, 2010, **2**, 944-948.
11. M. P. Suh, H. J. Park, T. K. Prasad and D.-W. Lim, *Chemical Reviews*, 2011, **112**, 782-835.
12. D. Fairen-Jimenez, Y. J. Colón, O. K. Farha, Y.-S. Bae, J. T. Hupp and R. Q. Snurr, *Chemical Communications*, 2012, **48**, 10496-10498.
13. O. K. Farha, I. Eryazici, N. C. Jeong, B. G. Hauser, C. E. Wilmer, A. A. Sarjeant, R. Q. Snurr, S. T. Nguyen, A. Ö. Yazaydin and J. T. Hupp, *Journal of the American Chemical Society*, 2012, **134**, 15016-15021.
14. J. Goldsmith, A. G. Wong-Foy, M. J. Cafarella and D. J. Siegel, *Chemistry of Materials*, 2013, **25**, 3373-3382.
15. N. S. Bobbitt, J. Chen and R. Q. Snurr, *The Journal of Physical Chemistry C*, 2016, **120**, 27328-27341.
16. D. A. Gómez-Gualdrón, T. C. Wang, P. García-Holley, R. M. Sawelewa, E. Argueta, R. Q. Snurr, J. T. Hupp, T. Yildirim and O. K. Farha, *ACS Applied Materials & Interfaces*, 2017, **9**, 33419-33428.
17. Q. Yang and C. Zhong, *The Journal of Physical Chemistry B*, 2005, **110**, 655-658.
18. M. Dinca and J. R. Long, *Angew. Chem. Int. Ed.*, 2008, **47**, 6766-6779.
19. K. L. Mulfort, O. K. Farha, C. L. Stern, A. A. Sarjeant and J. T. Hupp, *J. Am. Chem. Soc.*, 2009, **131**, 3866-3868.
20. K. L. Mulfort, T. M. Wilson, M. R. Wasielewski and J. T. Hupp, *Langmuir*, 2009, **25**, 503.
21. D. Himsl, D. Wallacher and M. Hartmann, *Angew. Chem. Int. Ed.*, 2009, **48**, 4639-4642.
22. Z. Xiang, D. Cao, W. Wang, W. Yang, B. Han and J. Lu, *The Journal of Physical Chemistry C*, 2012, **116**, 5974-5980.
23. R. C. Lochan and M. Head-Gordon, *Physical Chemistry Chemical Physics*, 2006, **8**, 1357-1370.
24. Y. Y. Sun, Y.-H. Kim and S. B. Zhang, *J. Am. Chem. Soc.*, 2007, **129**, 12606-12607.
25. R. C. Lochan, R. Z. Khaliullin and M. Head-Gordon, *Inorganic Chemistry*, 2008, **47**, 4032-4044.
26. K. Sumida, D. Stück, L. Mino, J.-D. Chai, E. D. Bloch, O. Zavorotynska, L. J. Murray, M. Dincă, S. Chavan and S. Bordiga, *Journal of the American Chemical Society*, 2013, **135**, 1083-1091.
27. M. T. Kapelewski, S. J. Geier, M. R. Hudson, D. Stück, J. A. Mason, J. N. Nelson, D. J. Xiao, Z. Hulvey, E. Gilmour and S. A. FitzGerald, *Journal of the American Chemical Society*, 2014, **136**, 12119-12129.
28. E. Tsivion, J. R. Long and M. Head-Gordon, *Journal of the American Chemical Society*, 2014, **136**, 17827-17835.
29. T. Banu, A. Ghosh and A. K. Das, *Chemical Physics Letters*, 2016, **658**, 140-145.
30. E. Klontzas, A. Mavrandonakis, E. Tylianakis and G. E. Froudakis, *Nano Lett.*, 2008, **8**, 1572.
31. E. Klontzas, A. Mavrandonakis, E. Tylianakis and G. E. Froudakis, *Nano Letters*, 2008, **8**, 1572.
32. E. Tylianakis, E. Klontzas and G. E. Froudakis, *Nanotechnology*, 2009, **20**, 204030.
33. R. B. Getman, J. H. Miller, K. Wang and R. Q. Snurr, *J. Phys. Chem. C*, 2011, **115**, 2066-2075.
34. S. K. Brand, Y. J. Colón, R. B. Getman and R. Q. Snurr, *Microporous and Mesoporous Materials*, 2013, **171**, 103-109.
35. Y. J. Colón, S. K. Brand and R. Q. Snurr, *Chemical Physics Letters*, 2013, **577**, 76-81.
36. Y. J. Colón, D. Fairen-Jimenez, C. E. Wilmer and R. Q. Snurr, *The Journal of Physical Chemistry C*, 2014, **118**, 5383-5389.
37. Y. J. Colón, R. Krishna and R. Q. Snurr, *Microporous and Mesoporous Materials*, 2014, **185**, 190-196.
38. E. Tsivion, S. P. Veccham and M. Head-Gordon, *ChemPhysChem*, 2017, **18**, 184-188.
39. M. J. Frisch, G. W. Trucks, H. B. Schlegel, G. E. Scuseria, M. A. Robb, J. R. Cheeseman, G. Scalmani, V. Barone, B. Mennucci, G. A. Petersson, H. Nakatsuji, M. Caricato, X. Li, H. P. Hratchian, A. F. Izmaylov, J. Bloino, G. Zheng, J. L. Sonnenberg, M. Hada, M. Ehara, K. Toyota, R. Fukuda, J. Hasegawa, M. Ishida, T. Nakajima, Y. Honda, O. Kitao, H. Nakai, T. Vreven, J. J. A. Montgomery, J. E. Peralta, F. Ogliaro, M. Bearpark, J. J. Heyd, E. Brothers, K. N. Kudin, V. N. Staroverov, T. Keith, R. Kobayashi, J. Normand, K. Raghavachari, A. Rendell, J. C. Burant, S. S. Iyengar, J. Tomasi, M. Cossi, N. Rega, J. M. Millam, M. Klene, J. E. Knox, J. B. Cross, V. Bakken, C. Adamo, J. Jaramillo, R. Gomperts, R. E. Stratmann, O. Yazyev, A. J. Austin, R. Cammi, C. Pomelli, J. W. Ochterski, R. L. Martin, K. Morokuma, V. G. Zakrzewski, G. A. Voth, P. Salvador, J. J. Dannenberg, S. Dapprich, A. D. Daniels, O. Farkas, J. B. Foresman, J. V. Ortiz, J. Cioslowski and D. J. Fox, Gaussian, Inc., Wallingford, CT, Revision D.01 edn., 2013.
40. Y. Zhao and D. G. Truhlar, *Theor. Chem. Acc.*, 2008, **119**, 525.
41. S. F. Boys and F. Bernardi, *Molecular Physics*, 2002, **100**, 65-73.
42. W. Joseph and D. Ochterski Ph, *Thermochemistry in Gaussian*, <http://gaussian.com/wp-content/uploads/dl/thermo.pdf>, Accessed November 2017.
43. F. Weinhold, *Discovering chemistry with natural bond orbitals*, John Wiley & Sons, 2012.
44. Glendening E. D., Reed A. E., Carpenter J. E. and Weinhold F., *NBO 3.0 Program Manual*, <http://www.ccl.net/cqa/software/NT/mopac6/nbo.htm>, Accessed November 2017.
45. F. Weinhold and E. D. Glendening, *NBO 6.0 Program Manual*, [http://nbo6.chem.wisc.edu/nbo6ab\\_man.pdf](http://nbo6.chem.wisc.edu/nbo6ab_man.pdf), Accessed November 2017.
46. J. H. Cavka, S. Jakobsen, U. Olsbye, N. Guillou, C. Lamberti, S. Bordiga and K. P. Lillerud, *Journal of the American Chemical Society*, 2008, **130**, 13850-13851.



Quantum mechanical calculations provide insights into interactions between solvent molecules and metal alkoxides and resulting hydrogen bonding energies.